Second response to the comments of the Reviewer 1

Dear Reviewer.

Thank you for taking a time to review our manuscript.

We were trying to follow your suggestions.

In the following we address the comments of the reviewer point by point.

Reviewer write: "First, I do not consider necessary many of the analysis devoted to atomic oxygen direct recombination process. So Figures 2 and 3, and many of the discussion refereed to them, should not be here. Once the authors obtain from direct recombination analysis that an efficiency of 0.07-0.13 is required for O2(b) production means that this process, alone, can not explain O2(b) production …."

McDade et al. (1986) made the conclusion that one-step mechanism is not working not because their efficiency to high, but because it depends on altitude, that is impossible by the essence of ε. They are writing: "The altitude dependence of ε suggests that the observations are not consistent with the direct excitation mechanism unless the efficiency for $O_2\left(b^1\Sigma_g^+\right)$ formation is strongly temperature dependent."

Because our experiment is essentially differ (common volume observations) from former one, we should repeat the steps of McDade et al., (1986). Hence, figures 2, as well as short corresponding discussion should be saved. Please, approach with understanding.

Nevertheless, in order to satisfy the reviewer suggestions, we delete figure 3 and radically reduce the discussion of one-step mechanism and made it as short as it is possible.

Reviewer write:" …then, all additional the work of considering only direct recombination process and possible dependences of the efficiency with temperature and pressure is very speculative, first because of the large value of this efficiency and second because in the altitude range of the atmospheric region considered (~10km) there is not large variation of temperature and pressure condition (although they could reach +-50K and/or a few micro bars)."

The temperature enters into Eq. (2) via coefficients k_1, $k_2^{O_2}$, $k_2^{N_2}$ under the exponential and power functions, hence, even small fluctuations of temperature produce essential deviations.

Reviewer write: "Figure 4, 5 and 7 need some improvements:

1) Plot some subintervals in the vertical and horizontal axes.

2) There are points (data) only at about each 3 km. Points at each 1 km should be shown, although the error bars be shown only each 3 km.

3) Figure 3 shows very good fit between about 97 and 98 km (as I can guess in figure 3 without any subdivision!). It will be interesting to show in the same figure the temperature profile (with and appropriate temperature scale in the upper horizontal axis), and the number density to see how the structure of temperature and number density can affect the fitting."

We modify figures 4, 5 and 7 according your suggestions:

1) we plot some subintervals in the vertical and horizontal axes;

2) we prefer to use 3 km step at figures 4 and 5 (ex. Fig.5 and Fig. 7) because it is more appropriate to the volume emission observations (see Hedin et al., 2009);

3) we think that you mean figure 4, because the fit shown on figure 4, but not on figure 3. We bring our apologies that do not show in the same figure number density and temperature. This does not give any information how the structure of temperature and number density affects the fitting, because: there are three parameters O, T, M; eq. (4) non-linear, and the effects of these parameters not obvious; thus, we may not distinguish influences of different parameters. Moreover, this is not the subject of our paper and it led to defocusing.

Specific suggestions of the reviewer.

Abstract.

Reviewer write:" Line 19- 20: ",we derived the empirical fitting coefficients,....(0,0) in terms of the atomic oxygen concentrations." Delete "in terms of the atomic oxygen concentrations" To read: ",we derived the empirical fitting coefficients,....(0,0).""

Lines 19- 20 are changed according to Reviewer suggestion.

Line 25: *Reviewer write:" Simultaneous and true common volume measurements of all the parameters used in this derivation, i.e...." Change to: Simultaneous measurements of all the parameters involved in the theoretical calculation of the observed O2(b) emission, i.e...."*

“Common volume measurements” is a special term well known and generally accepted for in-situ observations. Hence, we should save this term. The rest of the sentence is modified according with Reviewer claim.

1. Introduction.

Reviewer write:” Line 33-35 Change: "particularly, by emissions in the Atmospheric Band that form the excited state of molecular oxygen O2(b)..." To read " particularly, by the emission of the Atmospheric Band which is produced by the emission of the excited state of molecular oxygen O2(b)..."
Lines39-40 Change "Lopez-Gonzales" to "Lopez-Gonzalez"
Line 66 Delete "O or"
Line 67 Change "by known" To read "and"
Line 67 add "values" to read " volume emission values"
Line 70 change "leads to the loss of self-consistency (e.g Murtagh et al., 1990)." To read "leads to some degree of uncertainty (e.g Murtagh et al., 1990)."
Line 70-71. Delete "and, consequently, to essential biases." To read "(e.g Murtagh et al., 1990)."
Line 73-74 Delete " real common volume in-situ measurements of these..." To read: "simultaneous measurements of these..."
Line 75-79 Change "chapter" To read "section"”

Lines 33-35 are changed according to Reviewer suggestion.
Lines 39-40 are corrected as Reviewer suggest.
Lines: 66-67. The sentence is rewritten more clearly.
Line: 67. The word “values” is added after the words “volume emission” as Reviewer suggest.
Line 70 is modified according with Reviewer suggestion.
Lines 70-71 are changed deleted by Reviewer suggestion.
Line: 74. We save “common volume” as special term (see answer above), but the rest the sentence is modified according with Reviewer wish.
Lines: 75-79. The word "chapter" is changed to "section" through the entire manuscript.

2. Rocket experiment description.

Reviewer write: "Here I have a question, it is described that FIPEX use two types of solid electrolyte sensors platinum electrodes sensitive to both molecular and atomic oxygen, whilst gold electrodes show a selective sensitivity to atomic oxygen. Is this mean that it can measure molecular oxygen too? If it is possible, It would be useful this O2 profile were shown in the plot."

We use the CONE number density measurements and partial partitioning from NRLMSISE-00 reference atmosphere (Picone et al., 2002). The FIPEX O_2 density measurements are not used: for reasoning and discussion see Eberhart et al. (2015). To avoid such confusion we rewrote the FIPEX experiment description.

3. Theory.

Reviewer write: "All this section is just a very detailed recompilation of the known mathematical expressions used in O2b calculations. There are too many details that should be reduced.
I think expression (2) should be deleted is already said in line 135-136 (same that equation 1).
Then expression (4) and (5) should be deleted and put only expression (6). Then delete expression (7), it is not needed, and write expression (8).
Then (1),(3), (6) and (8) expressions could be written, to easy understand the "nomenclature"."

All of Reviewer suggestions are applied. Equations (2), (4), (5), and (7) are deleted.

4. Results and Discussion.

Reviewer write: "Comment: Figure 1, shows atmospheric concentration, [N], temperature, T, atomic oxygen concentration, [O], and Volume emission rate. Here Figures 1b) and 1c) should have additional subintervals in the logarithmic x axis. Additionally molecular oxygen

concentration is used in the analysis performed. I have a question what values of O2 are used? (is there some additional measurement from FIPEX?, or are derived from the measurements of [N] (density) and [O]?)"

We add subintervals in Figure 1. Molecular oxygen is derived from CONE atmospheric number density measurements and partitioning from NRLMSISE-00 reference atmosphere (Picone et al., 2002). We add the notation into the section 2.

Reviewer write: "Question: Lines 174-177. It said: "Our rocket experiment shows an essential difference of emissions between ascending and descending flights (see Strelnikov et al., 2018). It also demonstrates a significant variability in other measured parameters, including neutral temperature and density as well as atomic oxygen density."
How large is this difference? The time between ascending and descending flights should be a very few minutes. Perhaps it could be interesting to show the profiles of the different parameters obtained in both, the ascending and descending, flights to see these differences."

We add the references where such difference is shown and discussed. Following Reviewer advice that the paper should have better focus we do not repeat this discussion in our manuscript.

4.1 One-step mechanism.

Reviewer write: "This subsection has to be very simplified. There is a lot of speculative exercise that leads to any point."

Situations in which the science allows a formulation of several reasonable alternatives, and it is impossible to show convincingly that only some one of them is right, are characteristic of all fields of scientific research. In this case researcher should discuss all available alternatives.

Reviewer write: "For example: The efficiency calculated by using direct atomic oxygen recombination for the production of O2b to explain the observed emission, is in the range of about 0.07-0.13, this value is too large compare with the obtained by laboratory and theoretical investigation (Wraight, 1982; Ogryzlo et al., 1984; Bates, 1988). Then, direct

atomic oxygen recombination alone can not explain the observed emission in agreement with earlier works (McDade et al., 1986; Bates, 1988;...)
Any other exercise is not necessary. So figure 2 y 3 should be deleted.".

As we discuss above, the figure 2 is saved but the section essentially simplified and figure 3 is deleted.

4.2 Two-step mechanism.

Reviewer write:" Figure 4. Please, put some subintervals specially in the y axis. Here I see a very good fitted region of about 97-98 km (as I guess because of the lack of subintervals!), and important deviation of the fit above and below this region. I think it would be interesting to show, simultaneously in the figure, T profile (with a horizontal scale from 150K to 210K, in the upper x axis) and the N profile (the same scale as RHS Eq.8, in the lower x axis, is appropriated) to easy see how temperature and atmospheric density profiles affect to the features observed in RHS equation 8."

To address the Reviewer's point we put subintervals in figure 4. T and M on figure 4 does not give an ability to see how the temperature and number density affects the RHS, because beside T and M there is third parameter (O) and one non-linear eq. (4) from which we may not distinguish influences of different parameters. Moreover, this is not the subject of our paper and it led to defocusing.

Reviewer write:
"Line 259: Delete "s" to read " and molecular oxygen"
Line 261: Change "are 3.1 and 2.9" to read "of 3.1 and 2.9"
Line 282-283 Change "we show Figure 5 with atomic oxygen concentration from... " To read "we compare in Figure 5 the atomic oxygen concentration from ..."
((Figure 5 and Figure 7 need to show subintervals in both axes (vertical and horizontal), also the data points should be plotted each 1 km.))"

Line: 259. "s" is deleted.
Line: 261. Changed.
Line: 282-283. Changed.

The subintervals in both axes at Figure 5 and Figure 7 (now Fig. 4 and Fig. 5) are added. We save resolutions 3 km as it is more relevant to volume emission observations.

4.3 Combined mechanism

Reviewer write:" Figure 6 is not necessary, all the information is in table 3."

This contradicts to (*). Nevertheless, in order to satisfy the Reviewer suggestion we delete Figure 6.

Reviewer write: "I do not think to put the equation (9) is needed. Neither do I consider an appendix necessary. So I will deleted the appendix and will reduce the equation 9 and the explanations to: "... we have investigated a combined mechanism of direct and indirect atomic oxygen recombination, the fitting coefficients for the transfer energy process were calculated for.... The results for the best-fit in each case are listed in Table 3." (Now in Table 3 only K3o/k3o2 and total efficiency would shown (delete D1 and D2)) "

We need this equation because it used to calculate fitting coefficients, hence, we have to show how it was derived, consequently, we save an appendix.

Reviewer write: "Line 305-310 Delete all.. "They are listed in Table 3. The altitude profile of the RHS of equation (9) and calculated fit-function are plotted in Figure 6. The deviations of fit function between limits and averaged values are negligible, hence, we only show the averaged case. Thus, we can recommend for future investigations the values of averaged case (last column of Tab. 3). Analogously to the two-step mechanism....<1.Taking into..." To read: "The results for the best-fit in each case are listed in Table 3.
Taking into..." "

This contradicts to (*) and (**). Nevertheless, in order to satisfy the suggestion of the Reviewer we delete lines 305-310 and add "The results for the best-fit in each case are listed in Table 3."

Reviewer write:" LIne 311. Add (see Table 3) to read "0.073 (see Table 3)."""

We add “(see Tab. 3)”.

Reviewer write:” Line 327-330. Delete this sentence "Note that... two point, respectively." It is not needed.”

This contradicts to (*). Nevertheless, in order to satisfy the suggestion of the Reviewer the sentences at lines 327-330 have been deleted.

Reviewer write:” Line 330-332. Rewrite this sentence. For example: The total efficiency of production of O2b through an energy transfer process and new coefficients derived in this work provide a valuable information about the chemistry of O2b. Moreover, the importance of make studies with the possibility of using simultaneous measurements is strongly pointed out.”

This contradicts to (*) and (**). Nevertheless, in order to satisfy the Reviewer the sentences were rewritten.

Conclusion.

Reviewer write: “This section has to be very summarised. There is a long text, and here the results has to be clearly established.”

Following by you suggestion the text of conclusion has been reduced.

Reviewer write: ”Line 336: Change "true common volume observations" to read "simultaneous observations". ”

“Common volume” is special term (see answer above). Trying to follow your suggestion we change "true common volume observations" to "common volume simultaneous observations".

Reviewer write: “Line 337-338 "delete one-step. two step and combined" to read "the mechanism of o2b formation were analysed".”

We delete “one-step. two step and combined” to “the mechanisms of $O_2\left(b^1\Sigma_g^+\right)$ formation were analysed.”

Reviewer write: "The following discussion for one-step and two-step should be deleted. These are from line 339 to 356. Only the proposed mechanism should be mentioned."

This contradicts to (*) and (**). In this paper we discus three mechanisms, hence, in conclusion should be highlighted all of them. Nevertheless, in order to satisfy the suggestion of the Reviewer we essentially reduce the conclusion owing to one-step mechanism.

Reviewer write: "Line 357-360 are when the main result are reflected. This can be rewritten as: Based on simultaneous observations of atomic oxygen, atmospheric band emission (762 nm), and density and temperature of the background atmosphere and all the information available up to now about reaction rates coefficients, branching ratios, quenching rates and spontaneous emission coefficients the mechanism of o2b formation were analysed.
A direct and indirect atomic oxygen recombination process to explain the production of O2(b) is the one chosen as responsible of the atmospheric emission observed. The total efficiency of production of O2b in the indirect recombination process is of 0.08 and the ratio of quenching coefficient of the precursor state is 0.231, when an efficiency of 0.02 in direct recombination is chosen. The analysis of the values of the total production indicates that O2A' or O2Pi may be possible precursors for the two-step mechanism."

We do not include the reviewer text instead of our conclusions because this contradicts to (*).

Reviewer write: "The lines 361-366 reflect the final thoughts, so here Lines 361-366 ramble on about these mechanisms again in a confused way. Instead, it should show the need to make simultaneous measurements to confirm and improve these results."

Note, lines 361-366 were written by authors. The Reviewer term *"ramble on about"* unacceptable. This contradicts to (*) and (**), hence, we save this formulation as it is. Nevertheless, in order to satisfy the suggestion of the Reviewer we include at the end of the conclusion the statement of the Reviewer about more simultaneous measurements in future to confirm and improve these results.

Thank you again.

With respect,

M. Grygalashvyly, M. Eberhart, J. Hedin, B. Strelnikov, F.-J. Lübken, M. Rapp, S. Löhle, S. Fasoulas, M. Khaplanov, J. Gumbel, and E. Vorobeva.

(*) 3. A referee of a manuscript should judge objectively the quality of the manuscript and respect the intellectual independence of the authors. In no case is personal criticism appropriate.

(**) 7. Referees should explain and support their judgements adequately so that editors and authors may understand the basis of their comments.

(General obligations for referees, ACP web page, https://www.atmospheric-chemistry-and-physics.net/for_reviewers/obligations_for_referees.html)

Response to the comments of the Reviewer 2

Dear Referee,

Thank you a lot for your constructive suggestions. We tried to follow your comments and suggestions. Please, approach with an understanding, that we should search a compromise between your suggestions and suggestions of other reviewers.

Specific comments.

Reviewer write: "1. It seems that there is an imbalance between the description of the three instruments used during the rocket mission. CONE and FIPEX are described in more or less detail, whereas for an Airglow Photometer only its functional purpose is mentioned. It is recommended to either shorten the description of the first two or expand the description of the Airglow Photometer."

We extend the description of the airglow photometer (lines 115-135 of the revised manuscript).

Reviewer write: "2. It is not clear why the theory is divided into two parts. It seems that the Appendix can be combined with the "Theory" section, and one should begin with the first sentence of the Appendix about the assumption of photochemical equilibrium. In this case, it is desirable to discuss the possibility of using the assumption of photochemical equilibrium at night. In addition, despite the well-established term "photochemical equilibrium", for pure night conditions it is more correct to call it "chemical equilibrium"."

We decided move derivation of equation for combined mechanism into Appendix in order to make the paper shorter and better focused. Now we discuss assumption about photochemical equilibrium at nigh directly in the section "Theory" (lines 174-178 of the revised manuscript). We use term photochemical equilibrium because it is more general and because even at night conditions exited molecular oxygen is a subject of sponateouse emission.

Reviewer write: "3. It is necessary to describe the method of estimating the errors shown in the figures. With such large errors, it is necessary to speak of height dependence of fraction of

recombination with caution. In addition, error estimates for the fitting coefficient estimates should also be presented."

The uncertainties were calculated with sensitivity analysis. We add some references where full description of this method is given (lines 231-233 of the revised manuscript). The discussion of Figure 2 and hight dependence has been modified taking into account large error (lines 238-241 of the revised manuscript). The uncertainties of the fitting coefficients for two-step mechanism, as well as for combined mechanism fitting coefficients are shown in the revised manuscript.

Reviewer write: "4. More detailed comparison to the McDade et al. (1986) fitting coefficients is desirable taking into account error analysis."

It is true that it is necessary to better inform potential readers about comparison with coefficients of McDade et al. (1986). Now we add such discussion at lines 254-264 of the revised manuscript (taking into account uncertainties), where, we hope, this subject is highlighted.

Technical corrections.

Reviewer write: "1. Figure captures should be extended. 2. Figure 3 is not correlation. 3. Equations (1) and (A2) are the same. After combing theory section and appendix some equations may be omitted."

All of your technical corrections were utilized.

1. The captions for all figures are extended.

2. Figure 3 has been deleted by the suggestion of Reviewer 1.

3. Here, we think you mean Eq. 4 and (A2). By the suggestions of Reviewer 1 Eq. 4 (as well as Eq. 2, 5, 7) has been deleted.

Other changes are related to the recommendations and demands of other referee. Thank you a lot for taking the time to review our manuscript.

With respect,

M. Grygalashvyly, M. Eberhart, J. Hedin, B. Strelnikov, F.-J. Lübken, M. Rapp, S. Löhle, S. Fasoulas, M. Khaplanov, J. Gumbel, and E. Vorobeva.

Response to the comments of the Reviewer 3

Dear Referee,

Thank you very much for your constructive suggestions. We tried to follow your comments and suggestions, but, please, approach with an understanding, that we should search a compromise between your suggestions and suggestions of other reviewers.

Major comments.

It is true that it is necessary to better inform potential readers about volume emission measurements. Now we add such description at lines 115-135 of the revised manuscript, where, we hope, all of your questions are highlighted.

Section 3.

We pointed out now directly in Section 3 that we consider combined mechanism in section 4.3 and derive an expression for corresponding fit-function in Appendix (lines 190-192 of the revised manuscript).

Now we mention in Sec. 3 that the assumptions about photochemical equilibrium for $O_2(b^1\Sigma)$ and O_2^* are used (lines l55-156, 171-172, and 174-178 of the revised manuscript) .

We add the notation that the coefficients C^O and C^{O2}, and consequently k_3, are assumed to be temperature independent (or dependence is weak) and short discussion of this assumption (lines 183-188 of the revised manuscript).

Line 194-196 (hereafter, line numbers at the beginning as in review), Figure 2.

The uncertainties were calculated according with sensitivity analysis. Now we mention this directly in the manuscript and give the references (lines 231-233 of the revised manuscript).

The sensitivity analysis allows to estimates uncertainty of target component on the basis of errors of parameters of given component. Advantage of the sensitivity analysis consists that it considers contribution of each parameter to uncertainty of target component at the expense of sensitivity coefficients.

In our case, the dependence of target component on parameters is known as well as the errors of these parameters. Thus, calculating all sensitivity coefficients (partial derivatives of target

components for each parameter), we define the resulting uncertainty of each target component.

Line 197. Information about ε taking into account both the variance and the error range has been included.

Line 198. The information about mean with error range based on the variance and error range of the individual points is provided.

Line 199-200. The corresponding discussion is corrected. Now we mark that considering the large error range, there is no significant altitude dependence and state in the paper that the variability of the data points is much smaller than the errors of the individual points (lines 238-241 of the revised manuscript).

Line 203. This is true. Considering our large errors, we can't really derive any evidence for functional dependence. By demand of 1st reviewer the figure 3 has been deleted, as well as corresponding discussion.

Line 235. We provide an error range based on error propagation from the error and variance of RHS as provided in Figure 3. Now we compare these values directly with the values given by McDade et al. (1986). Possible reasons for the large discrepancy in C^{O} are noted (lines 254-264 of the revised manuscript).

Line 238. We add the notation that the assumption $\left(k_3^{N_2} \ll k_3^{O_2}\right)$ is just working hypothesis which is commonly used for analysis of precursor and, currently, there is no any evidence, neither for nor against that. If it is not true any definite conclusion on precursor by known C^{O2} is not possible (lines 267-273 of the revised manuscript).

Line 238. The error range for αγ has been provided (line 273 of the revised manuscript).

Line 250. We provides η=αγ as symbol for total efficiency for two-step mechanism and $\tilde{\eta} \equiv \tilde{\alpha}\tilde{\gamma}$ total efficiency for two-step channel at combined mechanism at line 274 of the revised manuscript.

Line 257. We add consideration of uncertainty for total efficiency. At lower limit of uncertainty ($\gamma = 0.061/\alpha < 1$) the result is saved, and considering upper limit ($\gamma = 0.222/\alpha < 1$), only $O_2(^5\Pi_g)$ may serve as precursor (lines 292-294 of the revised manuscript).

Line 268. We provided an error range for C^O/C^{O2} ratio (line 305 of the revised manuscript).

Line 283. We add recommended discussion (lines 327-333 of the revised manuscript).

Line 316. Now we note directly in the paper that Figure 7 (now Figure 5) is rather a sanity check than a validation (line 360 of the revised manuscript). Unfortunately we do not have other independent observation in present time. We add a notation about the necessity more independent common volume in-situ measurements to validate this results (lines 372-373 of the revised manuscript).

Line 349. We add error range and made a statement how our values compare to previous of McDade et al. (1986) (lines 383-386 of the revised manuscript).

Line 358, 359. Now we provide the error range for these values (line 394 of the revised manuscript).

Minor comments.

All of your minor suggestions were utilized.
The text at lines 32-33 has been corrected. The lines 64-65 were reformulated more carefully.
We studied this work now and add into the reference list.

Other changes are related to the recommendations and demands of other referee. Thank you a lot for taking your time to review our manuscript.

With respect,
M. Grygalashvyly, M. Eberhart, J. Hedin, B. Strelnikov, F.-J. Lübken, M. Rapp, S. Löhle, S. Fasoulas, M. Khaplanov, J. Gumbel, and E. Vorobeva.

Atmospheric Band Fitting Coefficients Derived from Self-Consistent Rocket-Borne Experiment

Mykhaylo Grygalashvyly[1], Martin Eberhart[5], Jonas Hedin[4], Boris Strelnikov[1], Franz-Josef Lübken[1], Markus Rapp[1,2], Stefan Löhle[5], Stefanos Fasoulas[5], Mikhail Khaplanov[4†], Jörg Gumbel[4], and Ekaterina Vorobeva[3]

[1]Leibniz-Institute of Atmospheric Physics at the University Rostock in Kühlungsborn, Schloss-Str. 6, D-18225 Ostseebad Kühlungsborn, Germany

[2]Deutsches Zentrum für Luft- und Raumfahrt, Institut für Physik der Atmosphäre, Oberpfaffenhofen, Germany

[3]Department of Atmospheric Physics, Saint-Petersburg State University, Universitetskaya Emb. 7/9, 199034, Saint-Petersburg, Russia

[4]Department of Meteorology (MISU), Stockholm University, Stockholm, Sweden

[5]University of Stuttgart, Institute of Space Systems, Stuttgart, Germany

[†]Deceased

Abstract

Based on self-consistent rocket-borne measurements of temperature, densities of atomic oxygen and neutral air, and volume emission of the Atmospheric Band (762 nm) we examined the one-step and two-step excitation mechanism of $O_2(b^1\Sigma_g^+)$ for night-time conditions. Following McDade et al. (1986), we derived the empirical fitting coefficients, which parameterize the Atmospheric Band emission $O_2(b^1\Sigma_g^+ - X^3\Sigma_g^-)(0,0)$ ~~in terms of the atomic oxygen concentrations~~. This allows to derive atomic oxygen concentration from night-time observations of Atmospheric Band emission $O_2(b^1\Sigma_g^+ - X^3\Sigma_g^-)(0,0)$. The derived empirical parameters can also be utilised for Atmospheric Band modelling. Additionally, we derived fit function and corresponding coefficients for combined (one- and two-step)

mechanism. Simultaneous ~~and true~~ common volume measurements of all the parameters ~~used in this derivation~~ involved in the theoretical calculation of the observed $O_2(b^1\Sigma_g^+ - X^3\Sigma_g^-)(0,0)$ emission, i.e. temperature and density of the background air, atomic oxygen density, and volume emission rate, is the novelty and the advantage of this work.

1. Introduction

The mesopause region is essential to understand the chemical and physical processes in the upper atmosphere because this is region of coldest temperature (during summer at high latitudes) and highest turbulence in the atmosphere (e.g. Lübken, 1997), the region of formation of such phenomena as NLC and PMSE (e.g. Rapp and Lübken, 2004), the region of gravity waves (GWs) breaking and formation of secondary GWs (Becker and Vadas, 2018), as well as the region of coupling between mesosphere and thermosphere ~~atmospheric layers~~. This region is characterised by different airglow emissions and, particularly, by the emissions ~~in~~ of the Atmospheric Band ~~that form~~ which is produced by the excited state of molecular oxygen $O_2(b^1\Sigma_g^+)$. Airglow observation in the Atmospheric Band is a useful method to study dynamical processes in the mesopause region. There have been a number of reports of gravity waves (GWs) detection in this band (Noxon, 1978; Viereck and Deehr, 1989; Zhang et al., 1993). Planetary wave climatology has been investigated by the Spectral Airglow Temperature Imager (SATI) instrument (Lopez-Gonzalez et al., 2009). In addition, the parameters of tides have been reported from SATI (Lopez-Gonzalez et al., 2005) and High Resolution Doppler Imager (HRDI) observations (Marsh et al., 1999). In number of works Sheese et al. (2010, 2011) ~~Takahashi~~ inferred the temperature by Atmospheric Band observation ~~(Takahashi et al., 1990; 1992; 2011)~~. Furthermore, the response of mesopause temperature and atomic oxygen during major sudden stratospheric warming was studied

553 utilising Atmospheric Band emission by Shepherd et al. (2010). Various works have focused
554 on Atmospheric Band emission modelling with respect to gravity waves and tides (e.g.
555 Hickey et al., 1993; Leko et al., 2002; Liu and Swenson, 2003). The specific theory of the
556 gravity wave effects on $O_2(b^1\Sigma_g^+)$ emission was derived in Tarasick and Shepherd (1992).
557 Moreover, Atmospheric Band observations have been widely utilised to infer atomic oxygen,
558 which is an essential chemical constituent for energetic balance in the extended mesopause
559 region (e.g. Hedin et al., 2009, and references there in), and ozone concentration (Mlynczak et
560 al., 2001). Although there is a large field of application of Atmospheric Band emissions, there
561 is a lack of knowledge on processes of the $O_2(b^1\Sigma_g^+)$ population. Two main mechanisms of
562 night-time population (note, the day-time mechanisms are quite different, see e.g. Zarboo et
563 al., (2018)) were proposed: the first is the direct population from three-body recombination of
564 atomic oxygen (e. g. Deans et al., 1976); the second is the so-called two-step mechanism,
565 which assumes an intermediate excited precursor O_2^* (e. g. Witt et al., 1984; Greer et al.,
566 1981). It has been shown by laboratory experiments that the first mechanism alone has not
567 explained observed emissions (Young and Sharpless, 1963; Clyne at al., 1965; Young and
568 Black, 1966; Bates, 1988). The second mechanism entails a discussion about the precursor
569 excited state and additional ambiguities in their parameters (e.g. Greer et al., 1981; Ogryzlo et
570 al., 1984). Thus, Witt et al. (1984) proposed the hypothesis that the $O_2(c^1\Sigma_u^-)$ state is,
571 possibly, the precursor; López-González et al. (1992a) suppose that the precursor could be
572 $O_2(^5\Pi_g)$; Wildt et al. (1991) found by laboratory measurements that it could be $O_2(A^3\Sigma_u^+)$.
573 Hence, the problem of identification is still not solved. The ~~breakthrough~~ essential step in this
574 direction has been done after the ETON 2 (Energy Transfer in the Oxygen Nightglow) rocket
575 experiment. ETON 2 mission yielded empirical fitting parameters that allow either to quantify
576 the $O_2(b^1\Sigma_g^+)$ (and, consequently, volume emission) by known O, or atomic oxygen by
577 known volume emission values (McDade et al., 1986). Despite the significance of this work,

~~there was an ambiguity in the derived fitting parameters because~~ the temperature and density of air (necessary for derivation) were taken from CIRA-72 and MSIS-83 (Hedin, 1983) models. ~~which~~ This leads to ~~the loss of self-consistency~~ some degree of uncertainty (e.g. Murtagh et al., 1990) ~~and, consequently, to essential biases~~. Thus, more solid knowledge on these fitting coefficients based on consistent measurements of atomic oxygen, volume emission of Atmospheric Band, and temperature and density of background atmosphere is desirable. In this paper we present ~~real~~ common volume ~~in-situ~~ measurements of these parameters performed in the course of WADIS-2 sounding rocket mission. In the next section ~~chapter~~, we describe the rocket experiment and obtained data relevant for our study. In section ~~chapter~~ 3, to make the paper easier to understand, we repeat some theoretical approximations from McDade et al. (1986). The obtained results of our calculations are discussed in section ~~chapter~~ 4. Concluding remarks and summary are given in the last section ~~chapter~~.

2. Rocket experiment Description

The WADIS (Wave propagation and dissipation in the middle atmosphere: Energy budget and distribution of trace constituents) sounding rocket mission aimed to simultaneously study the propagation and dissipation of GWs and measure the concentration of atomic oxygen. It comprised two field campaigns conducted at the Andøya Space Center (ASC) in northern Norway (69°N, 16°E). The WADIS-2 sounding rocket was launched during the second campaign on 5 March 2015 at 01:44:00 UTC, that is, night-time conditions. For a more detailed mission description, the reader is referred to Strelnikov et al. (2017) and the accompanying paper by Strelnikov et al. (2018).

The WADIS-2 sounding rocket was equipped with the CONE instrument to measure absolute neutral air density and temperature with high spatial resolution, instrument for atomic oxygen

density measurements FIPEX (Flux Probe Experiment) and the Airglow Photometer for atmospheric band (762 nm) volume emission observation.

CONE (COmbined measurement of Neutrals and Electrons), operated by IAP (Leibniz Institute of Atmospheric Physics at the Rostock University), is a classical triode type ionisation gauge optimised for a pressure range between 10^{-5} to 1 mbar. The triode system is surrounded by two electrodes: Whilst the outermost grid is biased to +3 to +6 V to measure electron densities at a high spatial resolution, the next inner grid (-15 V) is meant to shield the ionisation gauge from ionospheric plasma. CONE is suitable for measureing absolute neutral air number densities at altitude range between 70 and 120 km. To obtain absolute densities, the gauges are calibrated in the laboratory using a high-quality pressure sensor, like a Baratron. The measured density profile can be further converted to a temperature profile assuming hydrostatic equilibrium. For a detailed description of the CONE instrument, see Giebeler et al. (1993) and Strelnikov et al. (2013). Molecular oxygen and molecular nitrogen are derived from CONE atmospheric number density measurements and partitioning according to NRLMSISE-00 reference atmosphere (Picone et al., 2002).

The Airglow Photometer operated by MISU (Stockholm University, Department of Meteorology) measures the emission of the molecular oxygen Atmospheric Band around 762 nm from the overhead column, from which volume emission rate is inferred by differentiation. For airglow measurements in general, a filter photometer is positioned under the nose cone viewing along the rocket axis with a defined field-of-view (FOV). For WADIS-2 however, the FOV of ±3° was tilted from the rocket axis by 3° to avoid having other parts of the payload within the FOV and at the same time roughly view the same volume as the other instruments. The optical design is a standard radiometer-type system with an objective lens, a field lens, aperture and stops which provide an even illumination over a large portion of the detector surface (photomultiplier tube) and a defined FOV. At the entrance of the photometer there is an interference filter with a passband of 6 nm centred at 762 nm. During ascent, after

the nosecone ejection, the photometer then counts the incoming photons from the overhead column (or actually the overhead cone). When the rocket passes through the layer the measured photon flux drops and above the emission layer only weak background emissions are present (e.g. the zodiacal and galactic light). After the profile has been corrected for background emissions and attitude (van Rhijn effect) it is converted from counts to radiance using pre-flight laboratory calibrations. The calibration considers the spectral shape of the 0-0 band of the $O_2\left(b^1\Sigma_g^+ - X^3\Sigma_g^-\right)(0,0)$ Atmospheric Band system and the overlap of the interference filter passband. The profile is then smoothed and numerically differentiated with respect to altitude to yield the volume emission rate of the emitting layer. The data were sampled with 1085 Hz which results in an altitude resolution of about 0.75 m during the passage of the airglow layer (the velocity was ~800m/s at 95 km). However, because of the high noise level, the profile needed to be averaged to a vertical resolution of at least 3 km in order to get satisfactory results after the differentiation. A more detailed description and review of this measurement technique is given by Hedin et al. (2009).

The aim of the FIPEX developed by the IRS (Institute of Space Systems, University of Stuttgart) is to measure the atomic oxygen density along the rocket trajectory with high spatial resolution. It employs ~~two types of~~ solid electrolyte sensor~~s that differ in their electrode material. Platinum electrodes are sensitive to both molecular and atomic oxygen, whilst gold electrodes show~~ which has a selective sensitivity to atomic oxygen. A low voltage is applied between anode and cathode pumping oxygen ions through the electrolyte ceramic (yttria stabilised zirconia). The current measured is proportional to the oxygen density. Sampling is realised with a frequency of 100 Hz and enables a spatial resolution of ~10 m. Laboratory calibrations were done for molecular and atomic oxygen. For a detailed description of the FIPEX instruments and their calibration techniques see Eberhart et al. (2015, 2018).

3. Theory

Here, we are repeating the theory of $O_2\left(b^1\Sigma_g^+ - X^3\Sigma_g^-\right)(0,0)$ night-time emissions following McDade et al. (1986) to make our paper more readable, ~~saving~~ using all nomenclature as in the original paper. All utilised reactions are listed in Table 1, together with corresponding reaction rates, branching ratios, quenching rates and spontaneous emission coefficients. Some components have been updated according to modern knowledge, thus, deviating from the work of McDade et al. (1986).

Assuming direct one-step mechanism as a main one for population and that the $O_2\left(b^1\Sigma_g^+\right)$ in photochemical equilibrium, we can write its concentration as a ratio of production to the loss term:

$$\left[O_2\left(b^1\Sigma_g^+\right)\right] = \frac{\varepsilon k_1 [O]^2 M}{A_2 + k_2^{O_2}[O_2] + k_2^{N_2}[N_2] + k_2^{O}[O]}, \quad (1)$$

where k_1 – reaction rate for three-body recombination of atomic oxygen, ε is the corresponding quantum yield of $O_2\left(b^1\Sigma_g^+\right)$ formation ~~fraction of recombination~~, A_2 represents the spontaneous emission coefficient, and $k_2^{O_2}, k_2^{N_2}, k_2^{O}$ are the quenching coefficients for reactions with O_2, N_2 and O, respectively.

~~The volume emission for transition $O_2\left(b^1\Sigma_g^+ - X^3\Sigma_g^-\right)(0,0)$ is a product of the concentration of excited molecules and the spontaneous emission coefficient for the given transition:~~

~~$$V_{at} = A_1\left[O_2\left(b^1\Sigma_g^+\right)\right] = \frac{A_1 \varepsilon k_1 [O]^2 M}{A_2 + k_2^{O_2}[O_2] + k_2^{N_2}[N_2] + k_2^{O}[O]}, \quad (2)$$~~

~~where A_1 is spontaneous emission for reaction R5 (hereafter, nomenclature RX means the reaction X from Table 1).~~ In case of known temperature, volume emission and concentrations of O, O_2, N_2, and M, the quantum yield of $O_2\left(b^1\Sigma_g^+\right)$ formation ~~fraction of recombination~~ can be calculated as follows:

$$\varepsilon = V_{at} \frac{A_2 + k_2^{O_2}[O_2] + k_2^{N_2}[N_2] + k_2^{O}[O]}{A_1 k_1 [O]^2 M}, \quad (2)$$

where A_1 is spontaneous emission for reaction R5 (hereafter, nomenclature RX means the reaction X from Table 1).

In the case of the two-step mechanism, the unknown excited state O_2^* is populated at the first step from the reaction R7. Then, it can be deactivated by quenching (R9), spontaneous emission (R10) or producing $O_2\left(b^1\Sigma_g^+\right)$ by the reaction R8. Note, R8 is one pathway of the overall quenching reaction R9. ~~The concentration of these excited molecules is given by the following expression:~~

~~$$[O_2^*] = \frac{\alpha k_1 [O]^2 M}{A_3 + k_3^{O_2}[O_2] + k_3^{N_2}[N_2] + k_3^{O}[O]}, \quad (4)$$~~

~~where fraction of recombination α, spontaneous emission coefficient A_3, quenching rates $k_3^{O_2}, k_3^{N_2}, k_3^{O}$ – are unknown values, as well as the precursor excited state.~~

In the second step, O_2^* is transformed into $O_2\left(b^1\Sigma_g^+\right)$, which, ~~in turn,~~ can be deactivated by quenching (R2-R4) and by spontaneous emission (R6). Assuming photochemical equilibrium for O_2^* and, as before, for $O_2\left(b^1\Sigma_g^+\right)$ ~~Its concentration in the case of the two-step mechanism is:~~

~~$$\left[O_2\left(b^1\Sigma_g^+\right)\right] = \frac{\gamma k_3^{O_2}[O_2][O_2^*]}{A_2 + k_2^{O_2}[O_2] + k_2^{N_2}[N_2] + k_2^{O}[O]}. \quad (5)$$~~

the volume emission in the case of $O_2\left(b^1\Sigma_g^+ - X^3\Sigma_g^-\right)(0,0)$ is:

$$V_{at} = \frac{A_1 \alpha k_1 [O]^2 M \gamma k_3^{O_2}[O_2]}{\left(A_2 + k_2^{O_2}[O_2] + k_2^{N_2}[N_2] + k_2^{O}[O]\right)\left(A_3 + k_3^{O_2}[O_2] + k_3^{N_2}[N_2] + k_3^{O}[O]\right)}, \quad (3)$$

where quantum yield of O_2^* formation α, quantum yield of $O_2\left(b^1\Sigma_g^+\right)$ formation γ, spontaneous emission coefficient A_3, and $k_3^{O_2}, k_3^{N_2}, k_3^{O}$ unknown quenching rates of O_2^*. Note, assumption about photochemical equilibrium for O_2^* and $O_2\left(b^1\Sigma_g^+\right)$ is valid, because $O_2\left(b^1\Sigma_g^+\right)$ radiative lifetime is less than 12 s and all potential candidates for of O_2^* have

lifetime less than several seconds (e.g. López-González et al., 1992a, 1992b, 1992c; Yankovsky et al., 2016, and references therein).

Collecting all known values on the right-hand side (RHS) and all unknown summands on the left-hand side (LHS), omitting emissive summand A_3 as non-effective loss (McDade et al., 1986) equation (3) can be rearranged as follows:

~~$$\frac{A_3 + k_3^{O_2}[O_2] + k_3^{N_2}[N_2] + k_3^{O}[O]}{\alpha\gamma k_3^{O_2}} = \frac{A_1 k_1 [O]^2 M[O_2]}{V_{at}\left(A_2 + k_2^{O_2}[O_2] + k_2^{N_2}[N_2] + k_2^{O}[O]\right)}.$$~~ ~~(7)~~

~~Omitting emissive summand A_3 as non-effective loss (McDade et al., 1986) we can transform (7) into the following expression:~~

$$C^{O_2}[O_2] + C^{O}[O] = \frac{A_1 k_1 [O]^2 M[O_2]}{V_{at}\left(A_2 + k_2^{O_2}[O_2] + k_2^{N_2}[N_2] + k_2^{O}[O]\right)}, \quad (4)$$

where $C^{O_2} = \left(1 + k_3^{N_2}[N_2]/k_3^{O_2}[O_2]\right)/\alpha\gamma$ and $C^{O} = k_3^{O}/\alpha\gamma k_3^{O_2}$ are the fitting coefficients that can be calculated by the least square fit (LSF) procedure. Such derivation assumes that the coefficients are temperature independent (or temperature dependence is weak). This means that the reaction rates k_3 are assumed to be temperature independent (dependence is weak), or have the same temperature dependency for all quenching partners (N_2, O_2, O). Currently, this statement on the basis of available information about potential precursors is submitted true, but for which the solid evidence is absent. We calculated them based on our measurements and will discuss the results in the following section ~~chapter~~.

In more general case population of $O_2\left(b^1\Sigma_g^+\right)$ occurs via both channels: one-step and two-step. We discuss such ability in section 4.3 and derive an expression for corresponding fit-function in Appendix.

4. Results and Discussion

Figure 1 shows input data for our calculations: temperature from CONE instrument (Fig. 1a), number density of air (Fig. 1b), atomic oxygen concentration measured by FIPEX (Fig. 1c) and volume emission at 762 nm from photometric instrument (Fig. 1d). A temperature minimum of ~158 K was observed at 104.2 km. A local temperature peak was measured at 98.9 km with values of 204.5 K. The secondary temperature minimum was visible at 95.4 km and amounted to ~173 K. Atomic oxygen concentration (Fig. 1c) had a peak of ~$4.7 \cdot 10^{11}$ [cm^{-3}] at 97.2 km and approximately coincided with the secondary temperature peak. The peak of volume emission was detected between 95 and 97 km with values of more than 1700 [$phot. \cdot cm^{-3} \cdot s^{-1}$]; this is slightly beneath the atomic oxygen corresponding maximum and slightly above the secondary temperature minimum. Note, this point to the competition of the temperature and the atomic oxygen concentration in the processes of atomic oxygen excited state $O_2(b^1\Sigma_g^+)$ formation. Independently of the mechanism of atmospheric band emission (Eq. 1 or Eq. 3), the numerator is directly proportional to the square of atomic oxygen concentration and inversely proportional to the third power of the temperature (via reaction rate k_1 and M, considering the ideal gas low). Our rocket experiment shows an essential difference of emissions between ascending and descending flights (see Strelnikov et al., 2018). It also demonstrates a significant variability in other measured parameters, including neutral temperature and density as well as atomic oxygen density (Strelnikov et al., 2017, 2018). This suggests that, in the case of the ETON 2 experiments, the temporal extrapolation of atomic oxygen for the time of the emission measurement flight (which was approximately 20 min earlier) may lead to serious biases in estimations because, as one can see from Eq. 1 and Eq. 3, volume emission depends on the atomic oxygen concentration quadratically. Since the best quality data were obtained during the descent of the WADIS-2 rocket flight, we chose this data set for our analysis (Strelnikov et al., 2018). The region above 104 km is subject to auroral contamination. In the region below 92 km, negative values may occur in the volume emission profile as the result of self-absorption in the denser atmosphere below the emission

layer. Hence, we considered the region near the peak of emission between 92 km and 104 km as most appropriate for our study. The comparisons of our measurements with other observations, as well as with the results of modelling are presented in several papers (e.g. Eberhart et al., 2018; Strelnikov et al., 2018).

4.1 One-step mechanism

Figure 2 shows the ~~fraction of recombination~~ quantum yield of $O_2(b^1\Sigma_g^+)$ formation ε calculated according to Eq. (2), which is necessary to form $O_2(b^1\Sigma_g^+)$ under the assumption that the direct three-body recombination of atomic oxygen is the main mechanism. The uncertainties for this figure (as well as for other figures) were calculated according with sensitivity analysis (von Clarmann, 2014; Yankovsky and Manuilova, 2018, (Appendix 1); Vorobeva et al., 2018). ~~As is expected, ε is scattered approximately~~ Calculated values of ε are placed in the range [0.07; 0.13], which is in good agreement with the values derived by McDade et al. (1986). The averaged value amounts to 0.11±0.018. The range of values taking into account both the variance and the error range amounts to [0.02; 0.22]. By the physical nature of this value, the ~~fraction of recombination~~ quantum yield of $O_2(b^1\Sigma_g^+)$ formation should not depend on altitude. Fig. 2 shows the ~~strong~~ some altitude dependence of central values of ε, but considering the large error range, there is no clear altitude dependence. The variability of the data points is much smaller than the errors of the individual points. Hence, in light of the analysis of our rocket experiment, we may not decline direct excitation mechanism. ~~Such behaviour of ε means that measured atmospheric emissions may not be explained merely in light of direct excitation mechanism if ε is independent of temperature.~~

~~Hence, we plot values of ε depending on measured temperature in Figure 3. The values are distributed not randomly and show clear functional dependence. This dependence has a~~

~~complex nonlinear form. The spiral shape points to the existence of a second parameter, which is probably the pressure. The reaction rates in general cases are the functions of temperature and pressure (e. g. Troe, 1979). Hence, ε, which represents the ratio of the reaction rates of different branches, must depend, in general, on temperature and pressure. Correct functional relation $\varepsilon = \varepsilon(T, p)$ can be obtained only through laboratory measurements. In light of the analysis of our rocket experiment, we can only state that such functional dependence may exist. Hence, an explanation of atmospheric band emission via one-step mechanism is, generally speaking, possible. On the other hand, an existence of functional dependence is the necessary but not sufficient condition to state that the one-step mechanism populates $O_2\left(b^1\Sigma_g^+\right)$. Moreover,~~ Although the population via one-step mechanism alone is, generally speaking, possible, it is improbable because laboratory experiments show that the direct excitation alone may not explain observed emissions (Young and Sharpless, 1963; Clyne at al., 1965; Young and Black, 1966; Bates, 1988). This conclusion is ~~partially~~ in agreement with the conclusion from McDade et al. (1986), which stated that the one-step excitation mechanism is not sufficient to explain the $O_2\left(b^1\Sigma_g^+\right)$ population.

~~The reason of some inconsistency between our and McDade et al. (1986) formulation is that, in the case of ETON 2 experiments it was not possible to correlate ε with the real temperature at the place and in time of rocket launch. For their analysis, mean temperature profiles were utilised from the models CIRA 72 and MSIS 83 (Hedin, 1983), which does not reproduce any short-time dynamical fluctuations, solar cycle conditions, etc. Hence, the investigation of correlation between temperature and ε was not possible. Therefore, just in frame of our experiment, we may not decline that $O_2\left(b^1\Sigma_g^+\right)$ is populated via one-step or other mechanisms, but taking into account the results of laboratory measurements Bates (1988) and theoretical investigations Wraight (1982), which infer too low ε (0.03 and 0.015, respectively)~~

~~we should conclude that one-step mechanism alone does not explain observed emissions.~~ Hence, in the following, we check the second energy transfer mechanism.

4.2 Two-step mechanism

Figure 3 depicts the altitude profile of the right hand side (RHS) of equation (4) and profile calculated by the least-square fit (LSF). The fitting coefficients, C^{O2} and C^{O}, resulting from this fit, ~~are~~ amount to $9.8^{-5.3}_{+6.5}$ and $2.1^{+0.3}_{-0.6}$, respectively. The uncertainties were calculated, as commonly for LSF (Bevington and Robinson, 2003), based on error propagation from the error and variance of RHS as provided in Figure 3. Our C^{O2} coefficient is partially, within the error range, in agreement with C^{O2} coefficients given in McDade et al. (1986), which amount to 4.8±0.3 and 6.6±0.4 for temperature from CIRA-72 and MSIS-83, respectively. The C^{O} coefficient is approximately one order lower. There are several possible reasons for the large discrepancy in C^{O}, for example the temperature dependence of the O-quenching or that, in the case of ETON 2 experiments mean temperature profiles from the models CIRA-72 and MSIS-83 were utilized, which does not reproduce any short-time dynamical fluctuations, solar cycle conditions, etc. In frame of our analysis, we may not identify the reason for the large discrepancy in C^{O} more precisely. Fitting coefficients defined in such a way (Eq. 4) do not have a direct physical meaning. However, they have a physical meaning in several limit cases. If the quenching coefficients of a precursor with molecular nitrogen are much smaller than those with molecular oxygen $\left(k_3^{N_2} \ll k_3^{O_2}\right)$, then $\alpha\gamma = 1/C^{O2}$. The assumption, that the quenching of the precursor with N_2 is much slower than quenching with O_2, is just working hypothesis, which is commonly used for analysis of possible precursor (e.g. McDade et al., 1986; López-González et al, 1992a, 1992b; and references therein). It is true for such potential precursor as $O_2(A^3\Sigma_u^+)$ (Kenner and Ogryzlo, 1983b), but generally, there is no evidence, neither for nor against that. If it is not true, any definite conclusion on precursor by known

C^{O2} is not possible. In our case $\alpha\gamma = 0.102^{+0.120}_{-0.041}$. In other words, in the case of two-step formation of $O_2(b^1\Sigma_g^+)$ with energy transfer agent O_2, the total efficiency $\eta = \alpha\gamma$ amounts to 10.2%, which is the lowest amongst known values. Based on rocket experiment data analysis (ETON), Witt et al. (1984) obtained $\alpha\gamma = 0.12 - 0.2$. According to McDade et al. (1986), for the case with $k_2^O = 8 \cdot 10^{-14}$, the total efficiencies are 0.15 and 0.21 for temperature profiles adopted from MSIS-83 and CIRA-72, respectively. The analyses of López-González et al. (1992a, c), adopted O_2, N_2, and temperature profiles from the model (Rodrigo et al., 1991), showed a total efficiency of 0.16. In contrast to our work, all investigations mentioned above utilised the temperature and atmospheric density from models which describe a mean state of the atmosphere. This is a possible reason for discrepancy in the results. Total efficiency η may serve as an auxiliary quantity to identify the precursor. According to the physical meaning of efficiency, it may not be larger than 1. Hence, α, γ, as well as the total efficiency are smaller than 1. Consequently, $\gamma = \eta/\alpha < 1$, and we can examine potential candidates for O_2^* with this criterion. From an energetic point of view, only four bound states of molecular oxygen can be considered as an intermediate state for the $O_2(b^1\Sigma_g^+)$ population: $O_2(A^3\Sigma_u^+), O_2(A'^3\Delta_u), O_2(c^1\Sigma_u^-)$, and $O_2(^5\Pi_g)$ (Greer et al., 1981; Wraight, 1982; Witt et al., 1984; McDade et al., 1986; López-González et al., 1992c). For better readability, we will partially repeat a table from López-González et al. (1992b, c) with known α in our work (Table 2). From Table 2, it can be seen that only $O_2(A'^3\Delta_u)$ and $O_2(^5\Pi_g)$ fit to the criterion of $\gamma = 0.102/\alpha < 1$. At lower limit of uncertainty ($\gamma = 0.061/\alpha < 1$) $O_2(A'^3\Delta_u)$ and $O_2(^5\Pi_g)$ satisfy to the criterion, and considering upper limit ($\gamma = 0.222/\alpha < 1$), only $O_2(^5\Pi_g)$ may serve as precursor.

The second expression that helps to clarify the choice of the precursor is the ratio of quenching rates. In the limit of low quenching with molecular nitrogen $(k_3^{N_2} \ll k_3^{O_2})$, the ratio of fitting coefficients equals the ratio of the quenching rates of atomic and molecular oxygens

$(C^O/C^{O2} = k_3^O/k_3^{O_2})$. An analysis from the ETON 2 rocket experiment yields values of quenching coefficients ratios of potential precursor ~~are~~ of 3.1 and 2.9 for temperatures from CIRA-72 and MSIS-83, respectively. This is close to the value from Ogryzlo et al. (1984), who found $k_3^O/k_3^{O_2} = 2.6$ by laboratory measurements; however, as was noted in their work, substitution of these values into the equation for emission yields 16 % of the observed emission (Ogryzlo et al., 1984). These findings point to the possibility of a too high measured ratio $k_3^O/k_3^{O_2}$ as the result of too strong quenching of precursor by atomic oxygen. Our value of quenching ratios $k_3^O/k_3^{O_2}$ amounts to $0.21^{+0.32}_{-0.12}$. There is not enough information on measured values for bound states of molecular oxygen. Laboratory measurements for $O_2(A^3\Sigma_u^+)(v = 0-4)$, $O_2(A^3\Sigma_u^+)(v = 2)$, and $O_2(c^1\Sigma_u^-)$ infer the values of $k_3^O/k_3^{O_2}$ ratio to be 30±30, 100±15, and 200±20, respectively (Kenner and Ogryzlo, 1980; Kenner and Ogryzlo, 1983a, 1983b; Kenner and Ogryzlo, 1984). On the other hand, Slanger et al. (1984) found a lower limit of $O_2(A^3\Sigma_u^+)(v = 8)$ quenching by O_2 must be $\geq 8 \cdot 10^{-11}$. If the results from Slanger et al. (1984) were applied to the results from Kenner and Ogryzlo (1980, 1984) for $k_3^{O_2}$, then the ratio of $k_3^O/k_3^{O_2}$would be two orders lower. This short discussion illustrates a strong scattering of this ratio. For our two potential candidates ($O_2(A'^3\Delta_u)$ and $O_2(^5\Pi_g)$), there is information about $k_3^O/k_3^{O_2}$ ratio for only $O_2(A'^3\Delta_u)$. Through the comprehensive analysis of known rocket experiments, López-González et al. (1992a, b, c) inferred that the upper limit of the ratio amounts to 1. Hence, our value of $k_3^O/k_3^{O_2} = 0.21^{+0.32}_{-0.12}$ agrees with this result. Consistent information from laboratory experiments on the ratio for $O_2(^5\Pi_g)$ is absent. Thus, we can propose as potential candidates for precursor both $O_2(A'^3\Delta_u)$ and $O_2(^5\Pi_g)$; however, we are not able to identify which of these two is more preferable.

In order to illustrate the application of the newly derived fitting coefficients we ~~show~~ compare in Figure 4 ~~with~~ the atomic oxygen concentration from FIPEX (black line), from NRL MSISE-00 reference atmosphere model (Picone et al., 2002) (red line); calculated with

McDade et al. (1986) coefficients (blue line), and with our fitting coefficients for the two-step mechanism (green line). In the region 94-98 km, i.e. at atomic oxygen peak and volume emission peak (see Fig. 1d) fitting coefficients from this paper better then McDade coefficients (MSIS-83 case) reproduce observed values. Our fitting coefficients and fitting coefficients of McDade give similar approximation above atomic oxygen peak (~98-104 km). The shape of the calculated profiles appears slightly different, with the peak maximum at a higher altitude than the observed. In this, our result resembles the McDade results, probably because in both cases, the ratio of two reaction rates is derived, but not the rates themselves. In the lower part our results and those of McDade differ, because our C^{O2} value is larger and term with molecular oxygen dominates. Nevertheless, the atomic oxygen retrieved with our fitting coefficients satisfactorily reproduces measurements, especially at the peak.

4.3 Combined mechanism

In the most general case, the $O_2(b^1\Sigma_g^+)$ population passes through two channels: directly and via precursor. In fact, theoretical calculations from Wraight (1982) and laboratory measurements from Bates (1988) predicted a direct population with efficiencies of 0.015 and 0.03, respectively, which is not sufficient to explain the observed emissions (Bates, 1988, Greer et al., 1981; Krasnopolsky, 1986). A similar value, ε=0.02, was shown in the analysis by López-González et al. (1992b, c). We investigated a combined mechanism based on the LSF calculation and fit function (derivation in Appendix):

$$\frac{[O_2]+D_1[O]}{D_2+\tilde{\varepsilon}(1+D_1[O]/[O_2])}=\frac{A_1k_1[O]^2M[O_2]}{V_{at}\left(A_2+k_2^{O_2}[O_2]+k_2^{N_2}[N_2]+k_2^{O}[O]\right)}, \quad (5)$$

where, hereafter, tildes denote that these are values for combined mechanism and do not equal to the values for one-step or two-step mechanisms (Sec. 4.1 and 4.2); $D_1=\tilde{k}_3^O/\tilde{k}_3^{O_2}$ and $D_2=\tilde{\alpha}\tilde{\gamma}$ are the fitting coefficients, which refer to the ratio of quenching rates and $\tilde{\eta}\equiv\tilde{\alpha}\tilde{\gamma}$

889 total efficiency for two-step channel, respectively. The fitting coefficients were calculated for
890 two limit cases $\tilde{\varepsilon}$=0.015 (Wraight, 1982), $\tilde{\varepsilon}$=0.03 (Bates, 1988) and for the averaged case
891 $\tilde{\varepsilon}$=0.022.
892 ~~They are listed in Table 3. The altitude profile of the RHS of equation (9) and calculated fit-~~
893 ~~function are plotted in Figure 6. The deviations of fit function between limits and averaged~~
894 ~~values are negligible, hence, we only show the averaged case. Thus, we can recommend for~~
895 ~~future investigations the values of averaged case (last column of Tab. 3).~~ The results for the
896 best-fit in each case are listed in Table 3. Analogously to the two-step mechanism (Sec. 4.2),
897 for the case of combined mechanism $\tilde{\gamma} = \tilde{\eta}/\tilde{\alpha} < 1$, ~~Taking into account the highest value for~~
898 ~~total efficiency,~~ hence, the precursor should satisfy $\tilde{\alpha} > 0.08^{+0.12}_{-0.04}$ (see Tab. 3). For central
899 values of $\tilde{\alpha}$, only $O_2(A'^3\Delta_u)$ and $O_2(^5\Pi_g)$ satisfy this criterion (see Tab. 2). At lower limit of
900 uncertainty ($\tilde{\alpha} > 0.04$) $O_2(A'^3\Delta_u)$, $O_2(A^3\Sigma_u^+)$, and $O_2(^5\Pi_g)$ satisfy to the criterion, and
901 considering upper limit ($\tilde{\alpha} > 0.2$), only $O_2(^5\Pi_g)$ may serve as precursor. The upper limit of
902 the ratio $k_3^O/k_3^{O_2} < 1$ for $O_2(A'^3\Delta_u)$, derived by López-González et al. (1992a, b, c), is in
903 agreement with our calculations ($0.231^{+0.358}_{-0.142}$). As it is noted above, the ratio for $O_2(^5\Pi_g)$ is
904 unknown. Consequently, taking into an account both conditions, only $O_2(A'^3\Delta_u)$ and
905 $O_2(^5\Pi_g)$ may serve as precursor.
906 Figure 5 illustrates a sanity check for volume emissions derived (black lines) with fitting
907 coefficients of McDade et al. (1986) for MSIS-83 (Fig. 5c) case and CIRA-72 case (Fig. 5d),
908 and with our newly derived fitting coefficients for two-step (Fig. 5a) and combined ($\tilde{\varepsilon} =$
909 0.022) mechanisms (Fig. 5b) in comparison with measured one (red lines). All of derived
910 volume emission profiles (black lines) were calculated based on ~~the~~ the temperature,
911 concentration of surrounding air, and concentration of atomic oxygen from our rocket launch.
912 The calculations with combined mechanism (Eq. 5) and two-step energy transfer mechanism
913 (Eq. 4) give almost identical results. The results obtained with new fitting coefficients are in

satisfactory agreement with the measured volume emissions at the peak and above, whereas the McDade coefficients related to the temperature from CIRA-72 give better approximations below the volume emission peak (92 km). The coefficients of McDade related to the temperature from MSIS-83 are in better agreement with our results and are almost identical above the volume emission peak. ~~Note that both mechanisms with newly derived coefficients give three of five points in the vicinity of uncertainties of measured values (see Fig. 7a and Fig 7b), whereas McDade coefficients for MSIS-83 case (Fig. 7c) and for CIRA-72 (Fig. 7d) give just one and two point, respectively. Hence, we can recommend our newly derived coefficients either for a two-step energy transfer process or for combined mechanism. We consider combined mechanism more preferable as it is more general.~~ More independent common volume in-situ measurements are necessary to validate these results.

5. Summary and conclusions

Based on the rocket-born ~~true~~ common volume simultaneous observations of atomic oxygen, atmospheric band emission (762 nm), and density and temperature of the background atmosphere, the ~~one-step, two-step and combined~~ mechanisms of $O_2\left(b^1\Sigma_g^+\right)$ formation were analysed. Our calculations show that ~~in the case of the one-step mechanism the fraction of atomic oxygen recombination ε depends on altitude~~. ~~The one-step mechanism inferred the functional dependence of ε on temperature. It has a nonlinear character because the fraction of recombination ε, in general, depends on temperature and pressure. Nevertheless, we consider~~ one-step direct excitation ~~as~~ is less probable ~~for~~ by the reasons discussed above (Sec. 4.1). ~~In the context of the rocket experiment, we do not have a possibility to retrieve functional dependence $\varepsilon = \varepsilon(T, p)$, which poses a task for future laboratory measurements.~~

For the case of the two-step mechanism, we found new coefficients for fit function in accordance with McDade et al. (1986), based on self-consistent temperature, atomic oxygen

and volume emission observation. These coefficients amounted to $C^{O2}=9.8^{-5.3}_{+6.5}$ and $C^{O}=2.1^{+0.3}_{-0.6}$. C^{O2} coefficient is partially, within the error range, in agreement with C^{O2} coefficients given in McDade et al. (1986), and C^{O} coefficient is approximately one order lower. The general implication of these results is parameterisation of volume emission in terms of known atomic oxygen. This can be utilised either for atmospheric band volume emission modelling or for estimation of atomic oxygen by known volume emission. We identified two candidates for the intermediate state of O_2^*. Our results show that $O_2(A'^3\Delta_u)$ or $O_2(^5\Pi_g)$ may serve as a precursor.

Taking into account both channels of $O_2\left(b^1\Sigma_g^+\right)$ formation, we proposed a combined mechanism. In this case, atomic oxygen via volume emission or volume emission based on known atomic oxygen can be calculated by equation (5). Recommended fitting coefficients amounted to $D_1=0.231^{+0.358}_{-0.142}$ and $D_2=0.08^{+0.12}_{-0.04}$, with the efficiency of the direct channel as $\tilde{\varepsilon} = 0.022$. These coefficients have a meaning of total efficiency ($\tilde{\alpha}\tilde{\gamma}$) and a ratio of quenching coefficients ($\tilde{k}_3^O/\tilde{k}_3^{O_2}$) for the two-step channel. The analysis of their values indicates that $O_2(A'^3\Delta_u)$ and $O_2(^5\Pi_g)$ may serve as possible precursors for the two-step channel at combined mechanism. ~~Unfortunately,~~ In the context of our rocket experiment, we do not have the possibility to figure out which mechanism is true. Nevertheless, we consider the combined mechanism as more relevant to nature, because it has a higher generality. This conclusion does not contradict to the current point of view that the two-step mechanism is dominant because $\tilde{\varepsilon}$ is assumed to be 1.5-3 %. Moreover, it is possible that in the reality the mechanism is much more complex and it has multi-channel or more than two-step nature. Undoubtedly, more common volume simultaneous observations of the Atmospheric Band and the atomic oxygen concentrations would be desirable to confirm and improve these results.

Appendix.

We consider photochemical equilibrium for the night-time $O_2\left(b^1\Sigma_g^+\right)$ concentration. If $O_2\left(b^1\Sigma_g^+\right)$ is produced via both channels, the equilibrium concentration is given by the following expression:

$$\left[O_2\left(b^1\Sigma_g^+\right)\right] = \frac{\tilde{\varepsilon}k_1[O]^2M + \tilde{\gamma}\tilde{k}_3^{O_2}[O_2][O_2^*]}{A_2 + k_2^{O_2}[O_2] + k_2^{N_2}[N_2] + k_2^{O}[O]}, \quad (A1)$$

where the tilde denotes the combined mechanism, $A_1, k_1, k_2^{O_2}, k_2^{N_2}, k_2^{O}, \tilde{k}_3^{O_2}$ are the ratios for corresponding processes (see Tab. 1) and O_2^* is the unknown precursor.

Considering this precursor in photochemical equilibrium, we can obtain the following expression for its concentration:

$$[O_2^*] = \frac{\tilde{\alpha}k_1[O]^2M}{\tilde{A}_3 + \tilde{k}_3^{O_2}[O_2] + \tilde{k}_3^{N_2}[N_2] + \tilde{k}_3^{O}[O]}, \quad (A2)$$

where efficiency $\tilde{\alpha}$, $\tilde{A}_3$ is the unknown spontaneous emission coefficient of O_2^* and $\tilde{k}_3^{O_2}, \tilde{k}_3^{N_2}, \tilde{k}_3^{O}$ are the unknown quenching rates for O_2^*.

Substituting A2 into A1 and into expression for volume emission we obtain:

$$V_{at} = A_1\left[O_2\left(b^1\Sigma_g^+\right)\right] =$$

$$= \frac{A_1k_1[O]^2[O_2]M}{A_2 + k_2^{O_2}[O_2] + k_2^{N_2}[N_2] + k_2^{O}[O]}\left(\frac{\tilde{\varepsilon}}{[O_2]} + \frac{\tilde{\alpha}\tilde{\gamma}\tilde{k}_3^{O_2}}{\tilde{A}_3 + \tilde{k}_3^{O_2}[O_2] + \tilde{k}_3^{N_2}[N_2] + \tilde{k}_3^{O}[O]}\right). \quad (A3)$$

We assume that, in analogy with two-step mechanism, a spontaneous emission $\widetilde{A_3}$ of O_2^* is much smaller than the quenching, and we utilised traditional assumption about low quenching with molecular nitrogen $\left(\tilde{k}_3^{N_2} \ll \tilde{k}_3^{O_2}\right)$, which is commonly used to analyse a potential precursor. In this case, A3 can be rearranged as follows:

$$\frac{[O_2] + \frac{\tilde{k}_3^{O}}{\tilde{k}_3^{O_2}}[O]}{\tilde{\alpha}\tilde{\gamma} + \tilde{\varepsilon}\left(1 + \frac{\tilde{k}_3^{O}}{\tilde{k}_3^{O_2}}[O]/[O_2]\right)} = \frac{A_1k_1[O]^2M[O_2]}{V_{at}\left(A_2 + k_2^{O_2}[O_2] + k_2^{N_2}[N_2] + k_2^{O}[O]\right)}. \quad (A4)$$

We defined unknown fitting coefficients $D_1 \equiv \tilde{k}_3^O / \tilde{k}_3^{O_2}$ and $D_2 \equiv \tilde{\alpha}\tilde{\gamma}$. Expression A4 was utilised to calculate them with LSF.

Acknowledgements.

The authors are thankful to Prof. Dr. V. A. Yankovsky, Prof. Dr. W. Ward, and PD Dr. G. R. Sonnemann for helpful suggestions and useful discussions. This work was supported by the German Space Agency (DLR) under grant 50 OE 1001 (project WADIS). The authors thank DLR-MORABA for their excellent contribution to the project by developing the complicated WADIS payload and campaign support together with the Andøya Space Center, as well as H.-J. Heckl and T. Köpnick for building the rocket instrumentation.

The rocket-borne measurements and calculated data shown in this paper are available via IAP's ftp server at ftp://ftp.iap-kborn.de/data-in-publications/GrygalashvylyACP2018.

References

Bates, D. R.: Excitation and quenching of the oxygen bands in the nightglow, *Planet. Space Sci.*, **36(9)**, 875-881, 1988.

Becker, E., and Vadas, S. L.: Secondary gravity waves in the winter mesosphere: Results from a high-resolution global circulation model, *J. Geophys. Res.*, **123**, 2605-2627, doi:10.1002/2017JD027460, 2018.

Bevington, P. R., and Robinson, D. K.: Data reduction and error analysis for the physical sciences, 3rd edition, published by McGraw-Hill Companies Inc., ISBN 0-07-247227-8, 2003.

Campbell, I. M. and Gray, C. N.: Rate constants for O(^{3}P) recombination and association with N(4S), Chem. Phys. Lett., **8**, 259, 1973.

von Clarmann, T.: Smoothing error pitfalls, *Atmos. Meas. Tech.*, **7**, 3023-3034, https://doi.org/10.5194/amt-7-3023-2014, 2014.

Clyne, M. A. A., Thrush, B. A., and Wayne, R. P.: The formation and reactions of metastable oxygen $\left(b^1\Sigma_g^+\right)$ molecules, *J. Photochem. Photobiol.*, **4**, 957, 1965.

Deans, A. J., Shepherd, G. G., and Evans, W. F. J.: A rocket measurement of the $O_2\left(b^1\Sigma_g^+ - X^3\Sigma_g^-\right)$ atmospheric band nightglow altitude distribution, *Geophys. Res. Lett.*, **3(8)**, 441-444, 1976.

Eberhart, M., Löhle, S., Steinbeck, A., Binder, T., and Fasoulas, S.: Measurement of atomic oxygen in the middle atmosphere using solid electrolyte sensors and catalytic probes, *Atmospheric Measurement Techniques*, **8**, 3701–3714, doi:10.5194/amt-8-3701-2015, 2015.

Eberhart, M., Löhle, S., Strelnikov, B., Fasoulas, S. and Lübken, F.-J. Hedin, J., Khaplanov, M., Gumbel, J.: Atomic oxygen number densities in the MLT region measured by solid electrolyte sensors on WADIS-2, *Atmospheric Measurement Techniques*, submitted, 2018.

Giebeler, J., Lübken, F.-J., and Nägele, M.: CONE – a new sensor for in-situ observations of neutral and plasma density fluctuations, ESA SP, Montreux, Switzerland, ESA-SP-355, 311–318, 1993.

Greer, R. G. H., Llewellyn, E. J., Solheim, B. H., and Witt, G.: The excitation of $O_2(b^1\Sigma_g^+)$ in the nightglow, *Planet. Space Sci.*, **29**, 383, 1981.

Hedin, A. E.: A revised thermospheric model based on mass spectrometer and incoherent scatter data: MSIS-83, *J. Geophys. Res.*, **88**, 10.170, 1983.

Hedin, J., Gumbel, J., Stegman, J., and Witt, G.: Use of O_2 airglow for calibrating direct atomic oxygen measurements from sounding rockets, *Atmos. Meas. Tech.*, **2**, 801–812, 2009.

Hickey, M. P., Schubert, G., and Walterscheid, R. L.: Gravity wave-driven fluctuations in the O_2 atmospheric (0–1) nightglow from an extended, dissipative emission region, *J. Geophys. Res.*, **98**, 717–730, 1993.

Kenner, R. D. and Ogryzlo, E. A.: Deactivation of $O_2(A^3\Sigma_u^+)$ by O_2, O and Ar, *Int. J. Chem. Kinetics*, **12**, 501, 1980.

Kenner, R. D. and Ogryzlo, E. A.: Quenching of $O_2(c^1\Sigma_u^-, v=0)$ by O(^{3}P), $O_2(a^1\Delta_g)$ and other gases, *Can. J. Chem.*, **61**, 921, 1983a.

Kenner, R. D. and Ogryzlo, E. A.: Rate constant for the deactivation of $O_2(A^3\Sigma_u^+)$ by N_2, *Chem. Phys. Lett.*, **103**, 209, 1983b.

Kenner, R. D. and Ogryzlo, E. A.: Quenching of $O_2(A_{v=2} - X_{v=5})$ Herzberg I band by O_2(a) and O, *Can. J. Phys.*, **62**, 1599, 1984.

Krasnopolsky, V. A.: Oxygen emissions in the night airglow of the Earth, Venus and Mars, *Planet. Space Sci.*, **34**, 511, 1986.

Leko, J. J., M. P. Hickey, and Richards, P. G.: Comparison of simulated gravity wave-driven mesospheric airglow fluctuations observed from the ground and space, *J. Atmos. Solar-Terr. Phys.*, **64**, 397– 403, 2002.

Liu, A. Z. and Swenson, G. R.: A modeling study of O_2 and OH airglow perturbations induced by atmospheric gravity waves, *J. Geophys, Res.*, **108(D4)**, 4151, doi:10.1029/2002JD002474, 2003.

López-González, M. J., López-Moreno, J. J., and Rodrigo, R.: Altitude profiles of the atmospheric system of O_2 and of the green line emission, *Planet. Space Sci.*, **40(6)**, 783-795, 1992a.

López-González, M. J., López-Moreno, J. J., and Rodrigo, R.: Altitude and vibrational distribution of the O_2 ultraviolet nightglow emissions, *Planet. Space Sci.*, **40(7)**, 913-928, 1992b.

López-González, M. J., López-Moreno, J. J., and Rodrigo, R.: Atomic oxygen concentrations from airglow measurements of atomic and molecular oxygen emissions in the nightglow, *Planet. Space Sci.*, **40(7)**, 929-940, 1992c.

Lopez-Gonzalez, M. J., Rodríguez, E., Shepherd, G. G., Sargoytchev, S., Shepherd, M. G., Aushev, V. M., Brown, S., García-Comas, M., and Wiens, R. H.: Tidal variations of O_2

Atmospheric and OH(6-2) airglow and temperature at mid-latitudes from SATI observations, *Ann. Geophys.*, **23**, 3579–3590, 2005.

Lopez-Gonzalez, M. J., Rodríguez, E., García-Comas, M., Costa, V., Shepherd, M. G., Shepherd, G. G., Aushev, V. M., and Sargoytchev, S.: Climatology of planetary wave type oscillations with periods of 2-20 days derived from O_2 atmospheric and OH(6-2) airglow observations at mid-latitude with SATI, *Ann. Geophys.*, **27**, 3645–3662, 2009.

Lübken, F.-J.: Seasonal variation of turbulent energy dissipation rates at high latitudes as determined by in situ measurements of neutral density fluctuations, *J. Geophys. Res.*, **102**, 13,441-13,456, 1997.

McDade, I. C., Murtagh, D. P., Greer, R. G. H., Dickinson, P. H. G., Witt, G., Stegman, J., Llewellyn, E. J., Thomas, L., and Jenkins, D. B.: ETON 2: Quenching parameters for the proposed precursors of $O_2(b^1\Sigma_g^+)$ and $O(^1S)$ in the terrestrial nightglow, *Planet. Space Sci.*, **34**, 789–800, 1986.

Mlynczak, M. G., Morgan, F., Yee, J.-H., Espy, P., Murtagh, D., Marshall, B., Schmidlin, F.: Simultaneous measurements of the $O_2(^1\Delta)$ and $O_2(^1\Sigma)$ airglows and ozone in the daytime mesosphere, *Geophys. Res. Lett.*, **28**, 999-1002, 2001.

Murtagh, D. P., Witt, G., Stegman, J., McDade, I. C., Llewellyn, E. J., Harris, F., and Greer, R. G. H.: An assessment of proposed $O(^1S)$ and $O_2(b^1\Sigma_g^+)$ nightglow excitation parameters, *Planet. Space Sci.*, **38**, 1, 45–53, 1990.

Newnham, D. A. and Balard, J.: Visible absorption cross sections and integrated absorption intensities of molecular oxygen (O_2 and O_4), *J. Geophys, Res.*, **103(D22)**, 28801-28815, 1998.

Noxon, J. F.: Effect of Internal Gravity Waves Upon Night Airglow Temperatures, *Geophys. Res. Lett.*, **5**, 25–27, 1978.

Ogryzlo, E. A., Shen, Y. Q., and Wassel, P. T.: The yield of $O_2(b^1\Sigma_g^+)$ in oxygen atom recombination, *J. Photochem.*, **25**, 389, 1984.

Picone, J. M., Hedin, A. E., Drob, D. P., and Aikin, A. C.: NRLMSISE-00 empirical model of the atmosphere: Statistical comparisons and scientific issues, *J. Geophys, Res.*, **107**, 1468, doi:10.1029/2002JA009430, 2002.

Rapp. M, and Lübken, F.-J.: Polar mesosphere summer echoes (PMSE): Review of observations and current understanding, *Atmos. Chem. Phys.*, **4**, 2601-2633, 2004

Rodrigo, R., Lopez-Gonzalez, M. J., and Lopez-Moreno, J. J.: Variability of the neutral mesospheric and lower thermospheric composition in the diurnal cycle, *Planet. Space Sci.*, **39**, 803, 1991.

Sheese, P. E., Llewellyn, E. J., Gattinger, R. L., Bourassa, A. E., Degenstein, D. A., Lloyd, N. D., and McDade I. C.: Temperatures in the upper mesosphere and lower thermosphere from OSIRIS observations of O_2 A-band emission spectra, *Can. J. Phys.*, **88**, 919–925, doi:10.1139/P10-093, 2010.

Sheese, P. E., Llewellyn, E. J., Gattinger, R. L., Bourassa, A. E., Degenstein, D. A., Lloyd, N. D., and McDade I. C.: Mesopause temperatures during the polar mesospheric cloud season, *Geophys. Res. Lett.*, **38**, L11803, doi:10.1029/2011GL047437. 2011.

Shepherd, M. G., Cho, Y.-M., Shepherd, G. G., Ward, W., and Drummond, J. R.: Mesospheric temperature and atomic oxygen response during the January 2009 major stratospheric warming, *J. Geophys. Res.*, **115**, A07318, doi:10.1029/2009JA015172, 2010.

Slanger, T. G. and Black, G.: Interactions of $O_2(b^1\Sigma_g^+)$ with $O(^3P)$ and O_3. *J. Chem. Phys.*, **70**, 3434-3438, 1979.

Slanger, T. G., Bischel, W. K., and Dyer, M. J.: Photoexcitation of O_2 at 249.3 nm, *Chem. Phys. Lett.*, **108**, 472, 1984.

Smith, A. K., Marsh, D. R., Mlynczak, M. G., and Mast J. C.: Temporal variation of atomic oxygen in the upper mesosphere from SABER, *J. Geophys. Res.*, **115**, D18309, doi:10.1029/2009JD013434, 2010.

Smith, I. W. M.: The role of electronically excited states in recombination reactions, *Int. J. Chem. Phys.*, **16**, 423–443, 1984.

Strelnikov, B., Rapp, M., and Lübken, F.-J.: In-situ density measurements in the mesosphere/lower thermosphere region with the TOTAL and CONE instruments, in: An Introduction to Space Instrumentation, edited by: Oyama, K., Terra Publishers, doi:10.5047/isi.2012.001, 2013. http://www.terrapub.co.jp/onlineproceedings/ste/aisi/

Strelnikov, B., Szewczyk, A., Strelnikova, I., Latteck, R., Baumgarten, G., Lübken, F.-J., Rapp, M., Fasoulas, S., Löhle, S., Eberhart, M., Hoppe, U.-P., Dunker, T., Friedrich, M., Hedin, J., Khaplanov, M., Gumbel, J., and Barjatya, A.: Spatial and temporal variability in MLT turbulence inferred from in situ and ground based observations during the WADIS-1 sounding rocket campaign, *Ann. Geophys.*, **35**, 547–565, doi:10.5194/angeo-35-547-2017, 2017.

Strelnikov, B., Staszak, T., Strelnikova, I., Lübken, F.-J., Grygalashvyly, M., Hedin, J., Khaplanov, M., Gumbel, J., Fasoulas, S., Löhle, S., Eberhart, M., Baumgarten, G., Höffner, J., Wörl, R., Rapp, M., and Friedrich, M.: Simultaneous in situ measurements of small-scale structures in neutral, plasma, and atomic oxygen densities during WADIS sounding rocket project, *Atmos. Chem. Phys.*, submitted , 2018.

~~Takahashi, H., Sahai, Y., and Teixeira, N. R.: Airglow intensity and temperature response to atmospheric wave propagation in the mesopause region, *Adv. Space Res.*, **10**, 77–81, 1990.~~

~~Takahashi, H., Sahai, Y., Batista, P. P., and Clemesha, B. R.: Atmospheric gravity wave effect on the airglow O_2(0,1) and OH(9,4) band intensity and temperature variations observed from a low latitude station, *Adv. Space Res.*, **12(10)**, 131–134, 1992.~~

~~Takahashi, H., Onohara, A., Shiokawa, K., Vargas, F., Gobbi, D.: Atmospheric wave induced O_2 and OH airglow intensity variations: effect of vertical wavelength and damping, *Ann. Geophys*, **29**, 631–637, 2011.~~

Tarasick, D. W. and Shepherd, G. G.: Effects of gravity waves on complex airglow chemistries. 2. OH emission, *J. Geophys. Res.*, **97**, 3195-3208, 1992.

~~Troe, J.: Predictive Possibilities of Unimolecular Rate Theory, *J. Phys. Chem.*, **83 (1)**, 114-126, doi: 10.1021/j100464a019, 1979.~~

Viereck, R. A. and Deehr, C. S.: On the interaction between gravity waves and the OH Meinel (6-2) and O_2 Atmospheric (0-1) bands in the polar night airglow, *J. Geophys. Res.*, **94**, 5397–5404, 1989.

Vorobeva, E., Yankovsky, V., and Schayer, V.: Estimation of uncertainties of the results of [$O(^3P)$], [O_3] and [CO_2] retrievals in the mesosphere according to the YM2011 model by two approaches: sensitivity study and Monte Carlo method, EGU General Assembly, Vienna, Austria, 8–13 April 2018, EGU2018-AS1.31/ST3.7-17950, https://presentations.copernicus.org/EGU2018-17950_presentation.pdf, 2018.

Wildt, J., Bednarek, G., Fink, E. H., Wayne, R. P.: Laser excitation of the $A^3\Sigma_u^+$, $A'^3\Delta_u$ and $c^1\Sigma_{u-}$ states of molecular oxygen, *Chem. Phys.*, **156(3)**, 497-508, doi: 10.1016/0301-0104(91)89017-5, 1991.

Witt, G., Stegman, J., Murtagh, D. P., McDade, I. C., Greer, R. G. H., Dickinson, P. H. G., and Jenkins, D. B.: Collisional energy transfer and the excitation of $O_2(b^1\Sigma_g^+)$ in the atmosphere, *J. Photochem.*, **25**, 365, 1984.

Wraight, P. C.: Association of atomic oxygen and airglow excitation mechanisms, *Planet. Space Sci.*, **30(3)**, 251-259, 1982.

Yankovsky, V. A. and Manuilova, R. O.: Possibility of simultaneous [O_3] and [CO_2] altitude distribution retrievals from the daytime emissions of electronically-vibrationally excited molecular oxygen in the mesosphere, *J. Atmos. Sol.-Terr. Phys.*, **179**, 22-33, doi: 10.1016/j.jastp.2018.06.008, 2018.

Yankovsky, V. A., Martysenko, K. V., Manuilova, R. O., and Feofilov, A. G.: Oxygen dayglow emissions as proxies for atomic oxygen and ozone in the mesosphere and lower thermosphere, *J. Mol. Spectrosc.*, **327**, 209–231, doi:10.1016/j.jms.2016.03.006, 2016.

Young, R. A. and Sharpless, R. L.: Chemiluminescence and reactions involving atomic oxygen and nitrogen, *J. Chem. Phys.*, **39**, 1071, 1963.

Young, R. A. and Black, G.: Excited state formation and destruction in mixtures of atomic oxygen and nitrogen, *J. Chem. Phys.*, **44**, 3741, 1966.

Zagidullin, M. V., Khvatov, N. A., Medvedkov, I. A., Tolstov, G. I., Mebel, A. M., Heaven, M. C., and Azyazov, V. N.: $O_2(b^1\Sigma_g^+)$ Quenching by O_2, CO_2, H_2O, and N_2 at Temperatures of 300–800 K, *J. Phys. Chem.*, **121 (39)**, 7343-7348, doi: 10.1021/acs.jpca.7b07885, 2017.

Zarboo, A., Bender, S., Burrows, J. P., Orphal, J., and Sinnhuber, M.: Retrieval of $O_2(^1\Sigma)$ and $O_2(^1\Delta)$ volume emission rates in the mesosphere and lower thermosphere using SCIAMACHY MLT limb scans, *Atmos. Meas. Tech.*, **11**, 473-487, https://doi.org/10.5194/amt-11-473-2018, 2018.

Zhang, S. P., Wiens, R. H., and Shepherd, G. G.: Gravity waves from O_2 nightglow during the AIDA ‘89 campaign II: numerical modeling of the emission rate/temperature ratio, η, *J. Atmos. Terr. Phys.*, **55**, 377–395, 1993.

Table 1. List of reactions with corresponding reaction rates (for three-body reactions [cm^6 $molecule^{-2}$ s^{-1}] and for two-body reactions [cm^3 $molecule^{-1}$ s^{-1}]), quenching coefficients, and spontaneous emission coefficients (s^{-1}) used in the paper.

	Reaction	Coefficient	Reference
R1	$O + O + M \xrightarrow{\varepsilon k_1} O_2(b^1\Sigma_g^+) + M$	$k_1 = 4.7 \cdot 10^{-33}(300/T)^2$ $\varepsilon - unknown$	Campbel and Gray (1973)
R2	$O_2(b^1\Sigma_g^+) + O_2 \xrightarrow{k_2^{O_2}} products$	$k_2^{O_2} = 7.4 \cdot 10^{-17} T^{0.5} e^{-\frac{1104.7}{T}}$	Zagidullin et al. (2017)
R3	$O_2(b^1\Sigma_g^+) + N_2 \xrightarrow{k_2^{N_2}} products$	$k_2^{N_2} = 8 \cdot 10^{-20} T^{1.5} e^{\frac{503}{T}}$	Zagidullin et al. (2017)
R4	$O_2(b^1\Sigma_g^+) + O \xrightarrow{k_2^{O}} products$	$k_2^{O} = 8 \cdot 10^{-14}$	Slanger and Black (1979)
R5	$O_2(b^1\Sigma_g^+) \xrightarrow{A_1} O_2 + hv(762nm)$	$A_1 = 0.0834$	Newnham and Ballard (1998)
R6	$O_2(b^1\Sigma_g^+) \xrightarrow{A_2} O_2 + hv(total)$	$A_2 = 0.088158$	Yankovsky et al. (2016)
R7	$O + O + M \xrightarrow{\alpha k_1} O_2^* + M$	$\alpha - unknown$	
R8	$O_2^* + O_2 \xrightarrow{\gamma k_3^{O_2}} O_2(b^1\Sigma_g^+) + O_2$	$\gamma - unknown$	
R9	$O_2^* + O_2, N_2, O \xrightarrow{k_3^{O_2}, k_3^{N_2}, k_3^{O}} prod.$	$k_3^{O_2}, k_3^{N_2}, k_3^{O} - unknown$	
R10	$O_2^* \xrightarrow{A_3} O_2 + hv$	$A_3 - unknown$	

Table 2. Efficiencies α of the different excited states of O_2.

$O_2(c^1\Sigma_u^-)$	$O_2(A'^3\Delta_u)$	$O_2(A^3\Sigma_u^+)$	$O_2(^5\Pi_g)$	Reference
0.03	0.12	0.04	0.66	Wraight (1982), Smith (1984)
0.04	0.18	0.06	0.5	Bates (1988)
0.03	0.18	0.06	0.52	López-González et al. (1992a, b, c)

Table 3. Fitting coefficients for combined mechanism (Eq. 5) at different efficiencies.

	Low $\tilde{\varepsilon}$ Wraight (1982)	High $\tilde{\varepsilon}$ Bates (1988)	Averaged $\tilde{\varepsilon}$ (this work)
$\tilde{\varepsilon}$	0.015	0.03	0.022
$D_1 = \tilde{k}_3^O / \tilde{k}_3^{O_2}$	$0.211^{+0.355}_{-0.136}$	$0.397^{+0.22}_{-0.282}$	$0.231^{+0.358}_{-0.142}$
$D_2 = \tilde{\alpha}\tilde{\gamma}$	$0.087^{+0.12}_{-0.041}$	$0.073^{+0.119}_{-0.042}$	$0.08^{+0.12}_{-0.04}$

Figures.

Figure 1. Measurements of a) temperature (CONE), b) number density of air (CONE), c) atomic oxygen concentration (FIPEX), d) volume emission at 762 nm (photometer).

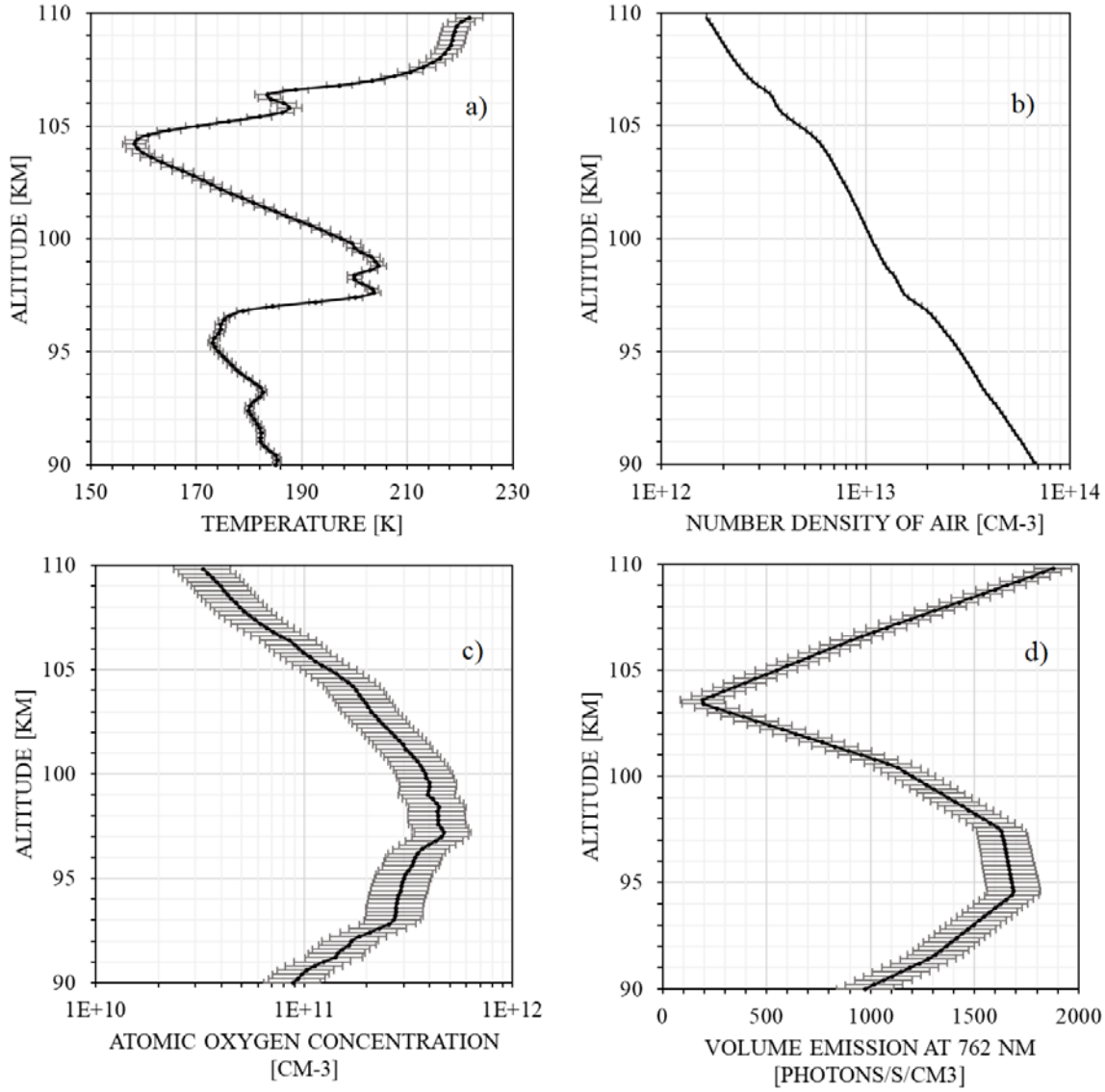

Figure 2. Quantum yield of $O_2(b^1\Sigma_g^+)$ formation ε for the case of one-step mechanism.

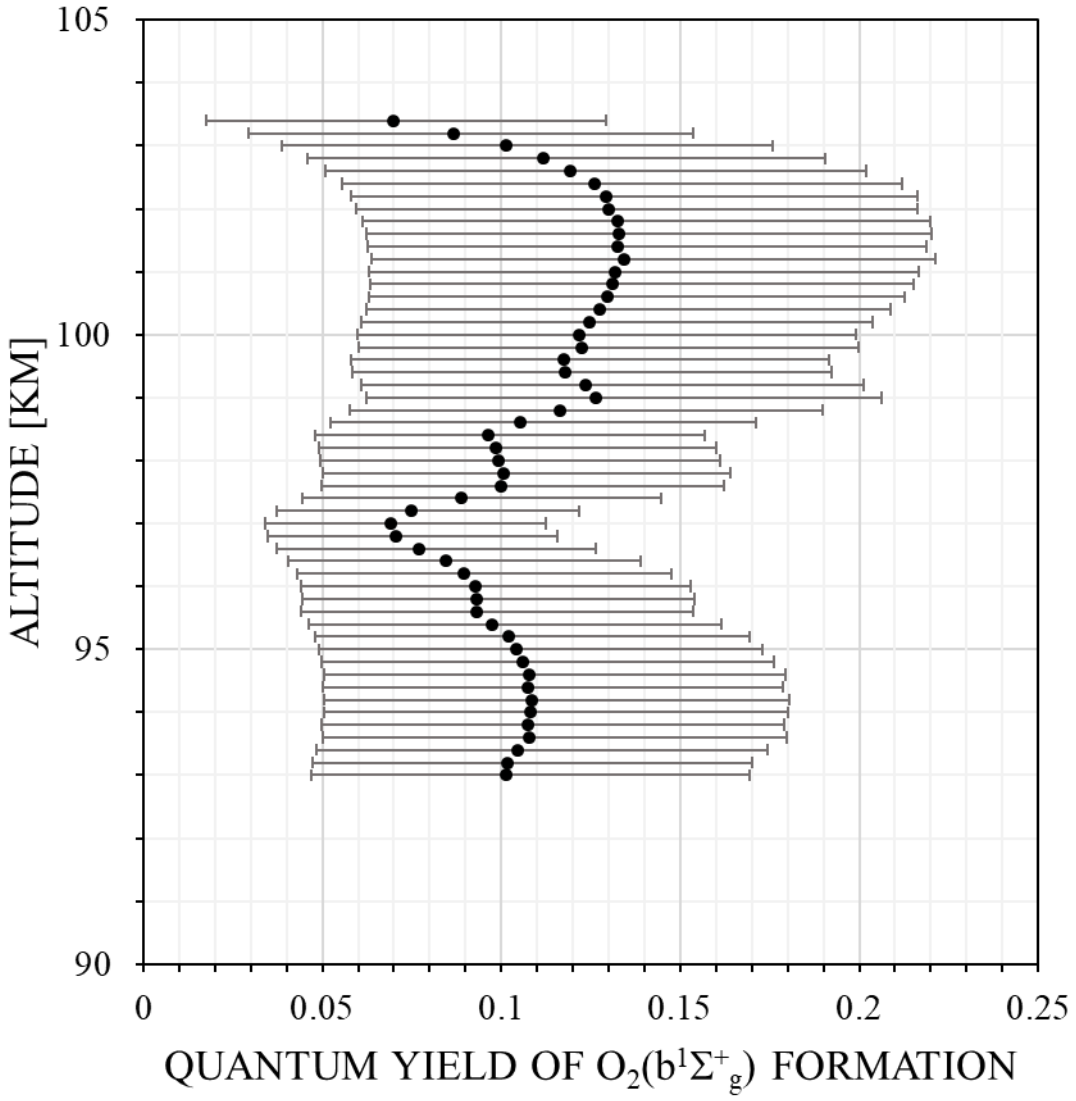

Figure 3. RHS (dots) and least-square fit of LHS (black line) of equation (4).

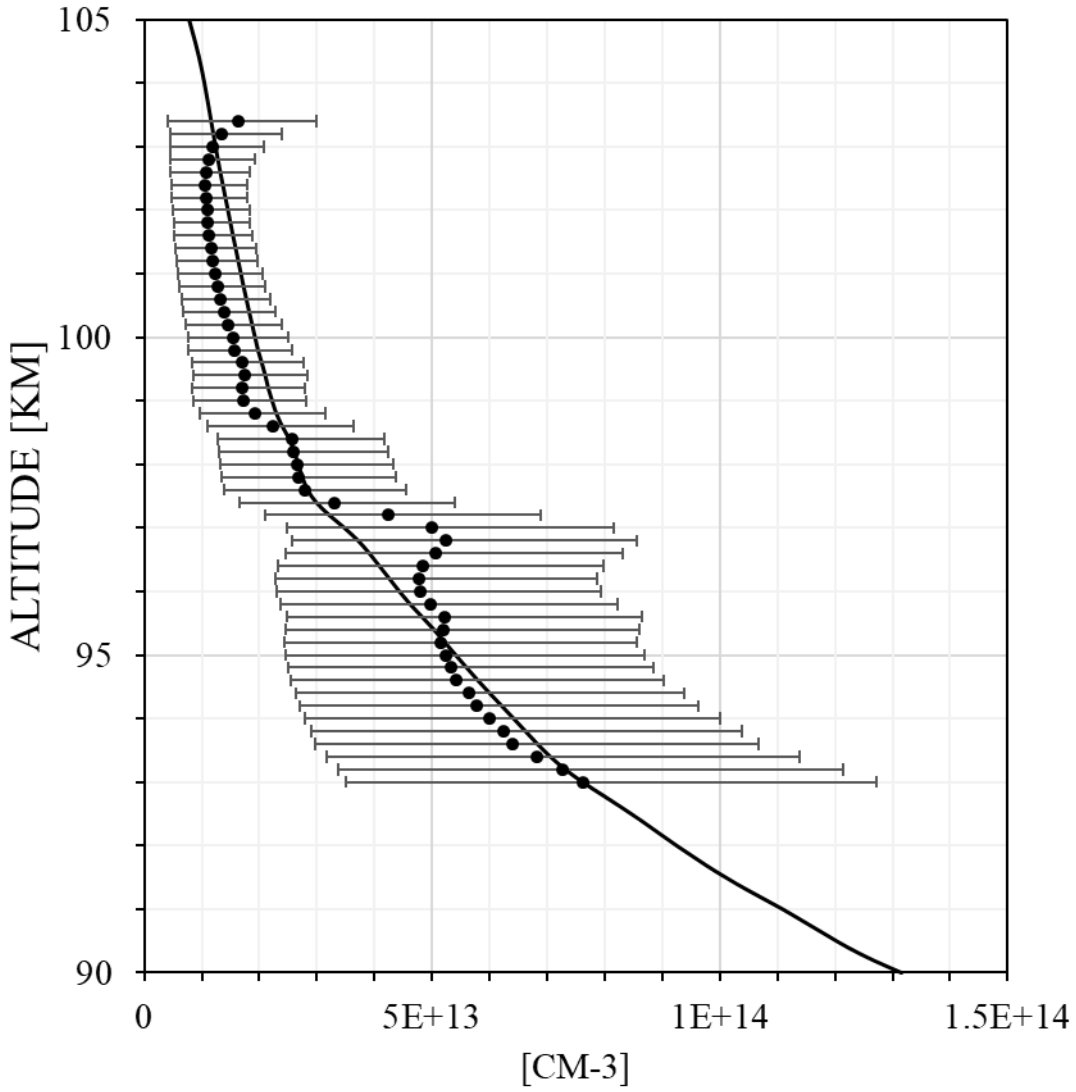

Figure 4. Atomic oxygen concentration: FIPEX (black line); model MSIS00 (red line); derived from emission observation with McDade et al. (1986) coefficients (blue line); calculated with newly derived fitting coefficients for the two-step mechanism (green line).

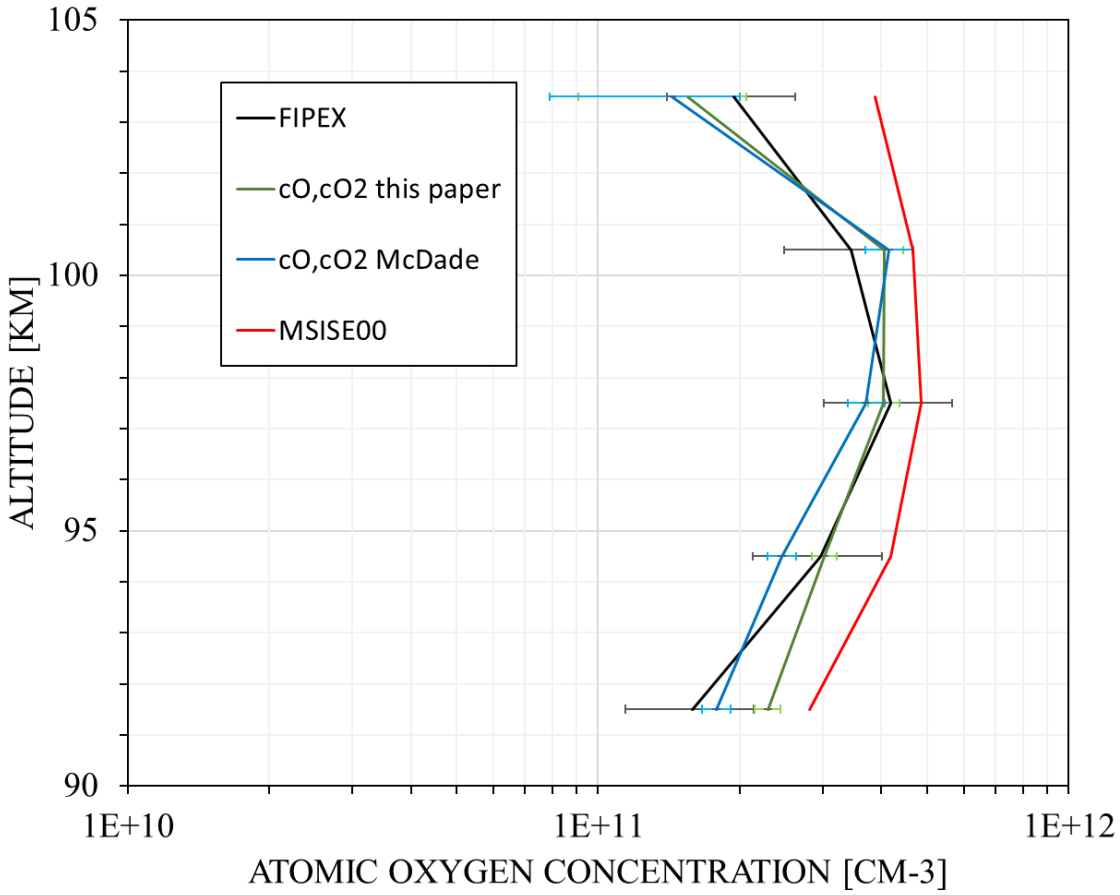

Figure 5. Volume emissions: photometer (red line); derived from atomic oxygen (black line) with a) newly derived fitting coefficients for the two-step mechanism, b) with fitting coefficients for combined mechanism, c) with McDade et al. (1986) coefficients, which correspond to the MSIS-83 temperature, and with McDade et al. (1986) coefficients, which correspond to the CIRA-72 temperatures.